

Lensless coherent imaging by sampling of the optical field with digital micromirror device

G. Vdovin,^{1,2,3} H. Gong,¹ O. Soloviev,^{1,3} P. Pozzi,¹ & M. Verhaegen¹

¹DCSC, TU Delft, Mekelweg 2, 2628CD, Delft, The Netherlands

²ITMO University, Kronverksky 49, 197101 St Petersburg, Russia

³Flexible Optical BV, Polakweg 10-11, 2288GG Rijswijk, the Netherlands

*g.v.vdovine@tudelft.nl

October 21, 2016

Abstract

We have experimentally demonstrated a lensless coherent microscope based on direct registration of the complex optical field by sampling the pupil with a sequence of two-point interferometers formed by the digital micromirror device. Complete registration of the complex amplitude in the pupil of imaging system, without any reference beam, provides a convenient link between the experimental and computational optics. Unlike other approaches to digital holography, our method does not require any external reference beam, resulting in a simple and robust registration setup. Computer analysis of the experimentally registered field allows for focusing the image in the whole range from zero to infinity, and for virtual correction of the aberrations present in the real optical system, by applying the adaptive wavefront corrections to its virtual model.

Keywords: Microscopy, Digital holography, Inverse problems, Phase retrieval, Adaptive optics

Reconstruction of the object by methods of digital holography [1] requires the complex amplitude of the field to be known with high spatial resolution. Since direct registration of the optical complex amplitude is impossible, a number of indirect techniques have been developed. Methods of digital holography, including phase-shift interferometry [2–4] require the reference beam to be present in the system. Such reference beam can be internally generated by spatial filtering of a portion of the object beam [5, 6], or through the use of light from an empty area of the field of view [7]. Reconstruction of phase from the intensity of the diffracted field [8–10] generally represents an ill-posed problem, and requires some additional information about the object to be made available. Reconstruction of the wavefront without a reference beam is possible with Shack-Hartmann sensor [11]. Recent publication [12] describes a quadriwave lateral shearing interferometer for high-resolution field reconstruction. However, methods based on the phase reconstruction from wavefront tilts, usu-

ally reconstruct only the potential component of the phase, neglecting phase vortices. Also, a relatively uniform intensity distributions needs to be present in the plane of reconstruction. These two factors significantly limit the applicability of these methods to digital holography. Time multiplexing [13, 14] represents another useful approach to high resolution reconstruction of the complex fields. In this approach the complex amplitude is registered sequentially in different locations of the pupil. This is usually achieved through complex setups requiring a reference beam and a galvanometric or piezoelectric scanner.

In the present communication we propose an alternative and more straightforward time-multiplexed technique for sampling of the wavefront for registration of both the amplitude and the phase of the optical field. The technique operates without any reference beam and without any imaging lens or a microscope objective, providing micrometer-scale resolution, which is comparable to previously reported techniques [5–7, 12, 14]. Digital Micromir-

ror Device (DMD), initially developed by Texas Instruments for image projection, have been used as image plane sampling device in spectrometry and laser beam characterization [15, 16]. In this communication we describe the use of DMD for sampling the optical field in the pupil plane by series of Young’s interferometers, dynamically formed by the micromirrors of a DMD.

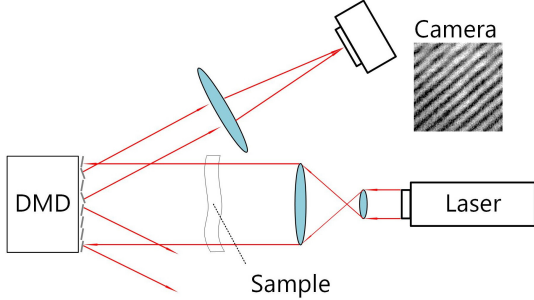


Figure 1: Coherent imaging setup based on field sampling with the use of DMD.

Figure 1 explains the principle of registration of the complex amplitude for the case of a transmissive object, however the same principle can be realized for reflective and scattering objects. The light beam emitted by laser and scattered by the object, forms a speckle pattern on the surface of DMD. The DMD device samples the field by turning on only two (reference and sample) micromirrors, to form a two-point interferometer. The fringe pattern is registered in the focal Fourier plane of the collective lens. The phase of the fringe pattern, with respect to the origin, is equal to the phase difference between the sample and reference micromirrors. The phase of the intensity pattern can be easily calculated by making a Fourier transform of the image, and then by calculating the phase in one of sidelobe maxima. The complete sequence, resulting in the registration of the complex amplitude of the field in all points corresponding to micromirrors with indices (i, j) and coordinates $x = i\delta$, $y = j\delta$, where δ is the pitch of the DMD, is given below:

- Chose reference micromirror, by scanning the intensity profile. To ensure high visibility of the interference pattern, the reference micromirror should be placed in an area with high intensity, for instance in a bright speckle. The reference micromirror stays in the “on” position during the whole registration process for all pixels in the aperture.
- Turn on the sample micromirror with coordinates (x, y) and register the interference pattern in the focal plane of the collective lens.

Example interferograms obtained with different micromirror pairs are shown in Fig. 2.

- Process the fringe pattern, to find the phase $\varphi_r(x, y)$ corresponding to the fundamental harmonic in the registered fringe pattern. This can be done by Fourier transforming the image and calculating the phase in one of two sidelobes. Register the intensity in the sample point $I_r(x, y)$ by calculating the total intensity in the registered fringe pattern.
- Go to the next sample micromirror, and proceed until field intensity and phase are registered for all points of interest.

Since all micromirrors, except the two that are used for interferometry, are in the “off” state, the reflected beam can be used for conventional imaging during the whole registration procedure.

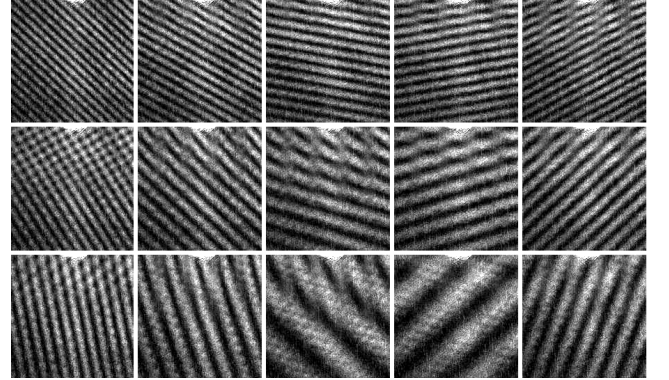


Figure 2: Interferograms obtained experimentally for different positions of the sampling micromirror.

The systematic phase errors are caused by the aberrations and misalignments in the path of the registration system, by the geometry of DMD, by the image noise and the limited size of the imaged area in the Fourier plane. The major systematic error is caused by the grating-like geometry of the DMD. The “on” pixels reflect incoming light at the angle of $\phi = 24^\circ$ in the sagittal (horizontal) plane, introducing path difference of $\Delta\varphi = x \sin(\phi) \approx 0.407x$ where x is the pixel coordinate in the sagittal plane. To enable a correct registration of the complex amplitude, the coherence length of the source L_c should satisfy the condition $L_c \gg 0.407A_x$, where A_x is the full size of the registered field in the sagittal plane.

To account for all systematic aberrations, we calibrated the system by measuring its response $\varphi_c(x, y)$ to a reference plane wave. Aligned stable system has to be calibrated only once. The intensity I_o and phase φ_o of the object field can be expressed

through the measured values of integral intensity of the interferogram $I_r(x, y)$ and phase $\varphi_r(x, y)$, and the phase of the calibration beam $\varphi_c(x, y)$:

$$\begin{aligned} I_o(x, y) &= I_r(x, y) - \min_{x,y}[I_r(x, y)] \\ \varphi_o(x, y) &= \varphi_r(x, y) - \varphi_c(x, y) \end{aligned} \quad (1)$$

The lateral resolution $r = 0.61\lambda/\text{NA}$ of the system is defined by its numerical aperture, which can be defined as $\text{NA} = A/2Z$, where A is the size of the virtual aperture, and Z is the distance between the DMD and the object. The numerical aperture of the virtual optical system can not be larger than the angle of diffraction on a single micromirror λ/δ , where we assume the micromirror size is equal to the pitch δ . With the smallest reported pitch of DMD of $5.4 \mu\text{m}$, and the wavelength varying in the range of $0.4 \dots 1.5 \mu\text{m}$, we obtain the NA range of $0.075 \dots 0.27$, with larger NA corresponding to a longer wavelength. In a similar way, the pixel pitch δ of the DMD determines the smallest spatial frequency detectable: λ/δ . Evidently, the field of view is limited by λ/δ as any two points separated by a larger angle would cause no interference.

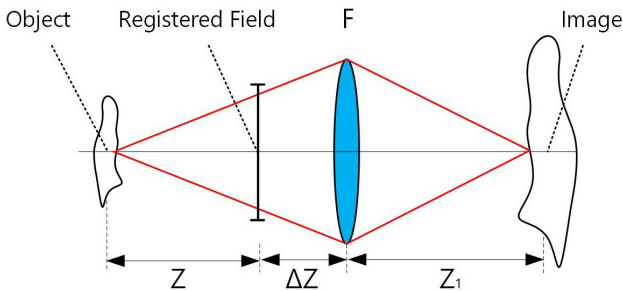


Figure 3: Virtual optical system for image reconstruction.

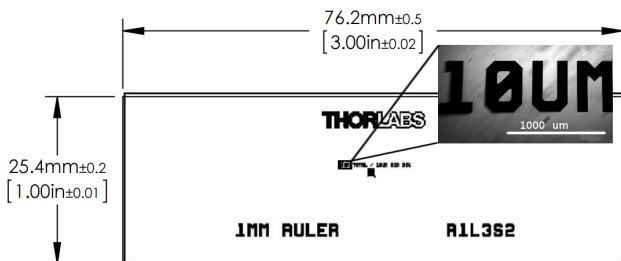


Figure 4: The object for imaging experiments: a stage micrometer (R1L3S2P) from Thorlabs. The central line (magnified in the inset) was used for experiments.

After the complex amplitude $U(x, y) = \sqrt{I_o(x, y)}e^{i\varphi_o(x, y)}$ is measured for all points in the pupil, the field distribution in the object plane

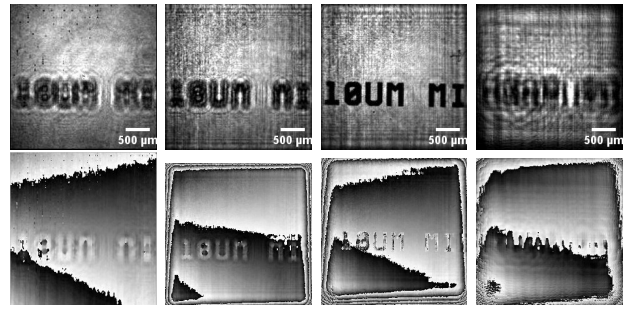


Figure 5: Field intensity (top) and phase (bottom) registered in different planes with magnification $M = 1$, and a total field of view of $3 \times 3 \text{ mm}$. From left to right the image shows fields registered at the DMD plane, and back propagated to -2.5 cm , -5.0 cm and -20.0 cm from the DMD.

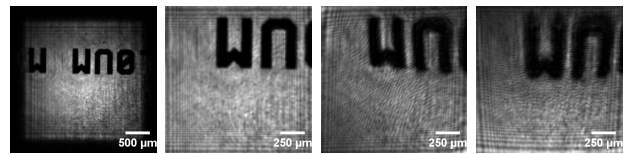


Figure 6: Image reconstructed in the best focus plane of a virtual optical system shown in Fig. 3, with magnification $M = -1$, with magnification $M = -2$, with $M = -2$ and one wave of astigmatism, and with $M = -2$ and one wave of coma (left to right).

can be reconstructed by direct back propagation from the plane of the DMD to the object plane, by using, for example, a spectral method:

$$\begin{aligned} U(x, y, Z) &= \Phi^{-1} \left[\Phi[U(x, y, 0)] \cdot e^{(-iZ\sqrt{k^2 - u_x^2 - u_y^2})} \right], \\ U(x, y, 0) &= \Phi^{-1} \left[\Phi[U(x, y, Z)] \cdot e^{(iZ\sqrt{k^2 - u_x^2 - u_y^2})} \right], \end{aligned} \quad (2)$$

where Φ and Φ^{-1} are forward and inverse Fourier transforms, Z is the distance from the object to the DMD, u_x and u_y are the coordinated in the Fourier space, and $k = 2\pi/\lambda$, where λ is the wavelength. Direct application of expressions (2) reconstructs the field with a magnification of $M = 1$. The magnification can be altered by propagation of the coherent field through a virtual optical system formed by a lens with focal length F , as shown in Fig. 3, where

$$\begin{aligned} M &= Z_1/(Z + \Delta Z), \\ F &= \frac{Z_1(Z + \Delta Z)}{Z_1 + Z + \Delta Z}. \end{aligned} \quad (3)$$

The lens can be modeled as a phase mask $\varphi_l(x, y) = k\frac{x^2 + y^2}{F}$. In the simplest case of $M = 1$ and $\Delta Z = 0$, we obtain $Z_1 = Z$, and $F = Z/2$.

Our experimental system is formed by a 15 mW He-Ne laser with a beam expander. The laser illuminates a low-cost DM365 “LightCrafter” DMD with a pixel pitch of $\delta = 10.8 \mu\text{m}$. The reflected light is collected to the Fourier plane by a two-inch F/3 lens with a focal length of 15 cm. The interferograms are registered by a low-cost CMOS camera with pixel pitch of $5.5 \mu\text{m}$ in a region of interest of 512×512 pixels. After registration of the reference phase, corresponding to undisturbed laser beam, an object represented by transparent glass slide (see Figure 4) with a high-resolution chrome mask was placed in the light path at a distance of ~ 5 cm from the DMD. The field was registered in a grid of 150×150 pixels, with pixel pitch of $2\delta = 21.6 \mu\text{m}$, forming a virtual square aperture of about 3×3 mm. The numerical aperture of the virtual optical system equals to $\text{NA} = A/2Z = 3/100 \sim 0.03$. The lateral resolution of the optical system is estimated as $r = 0.61\lambda/\text{NA} \sim 13\mu\text{m}$.

Figure 5 shows the field distribution registered in the plane of DMD, and reconstructed in three different planes, including the plane of best focus, by using back-propagation described by the pair of expressions (2). Figure 6 illustrates the result of propagation in a virtual optical system shown in Fig. 3 with $Z = \Delta Z = 0.05$ m, and magnification of $M = -1$ and $M = -2$. The last two images in Fig. 6 illustrate the possibility of virtual aberration correction by applying correcting phase terms to the experimentally registered complex field. Since the optical system is practically free from aberration, addition of aberration terms reduces the image sharpness, but proves the point that virtual adaptive correction is possible in such a system. Such a correction could be necessary, for example, if the object image is registered through the cover glass, causing spherical aberration.

Reconstruction of a complex field with dimensions of $N \times N$ requires N^2 interferograms to be registered and processed. Our experimental setup based on inexpensive components achieved registration rates of up to 7 pixels per second, mostly limited by the video interface of the DMD and the camera frame rate. Application of a more advanced DMD and camera would allow to increase the registration rate up to at least 4000 pixels per second, resulting in a time requirement of fifteen seconds per frame for pupil sampling of 256×256 pixels.

Further acceleration can be achieved by increasing the number of active pixel in a frame from two to a larger number, thus forming a sparse intensity mask in the pupil. Such a sparsely sampled pupil

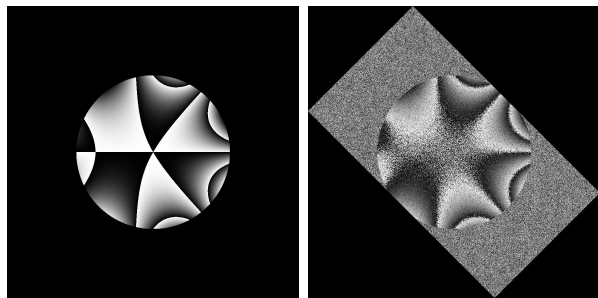


Figure 7: Original phase (left) and phase reconstructed from only 50 frames, using Gerchberg-Saxton algorithm.

produces speckle pattern in the image plane, which can be used for the reconstruction of the phase in all the “on” pixels at once, by solving the inverse problem, for instance using the Gerchberg-Saxton algorithm [8]. Our preliminary numerical experiments demonstrated full reconstruction of the phase in a pupil formed by 304×342 pixels from only 50 frames, with each frame randomly sampled with ~ 2100 pixels in the “on” state. Each frame with 2100 “on” pixels generated a single intensity pattern, limited to 255 scales of gray, to represent a 8-bit camera image. To obtain the common phase reference, one pixel was designated to be common between all 50 frames. The method yielded phase reconstruction, with only 10 iterations used in each frame. Such a quick convergence is conditioned by the randomness and sparsity of the intensity carrier in the pupil: in each frame only 2% of the total pixels are in the “on” state. An example of reconstruction of a low-order aberration introduced into a beam with uniform intensity distribution, is shown in Fig. 7. Although the first computational results are reassuring, a number of issues remains to be addressed in the future development: the speed of convergence, noise in the reconstruction, optimal choice of the common pixels etc. Also, in experiment, the propagation model used in the Gerchberg-Saxton algorithm should be calibrated, to take into account misalignments and aberrations of the system. Further development of the algorithm is possible by choice of a certain pattern for each frame in the sequence, for instance by using brighter pixels for the first frames, to speed up the collection of useful information. This approach would represent a kind of compressive sensing [17], which in our case will be employed not to the intensity field, but for the reconstruction of the complete complex field in the pupil of a coherent optical system. The work, aimed to further development of this approach, including its experimental implementation, is currently in

progress.

In conclusion, we have experimentally demonstrated registration of complex coherent optical field by aperture sampling using digital micromirror device. Unlike other approaches to digital holography, our method does not require any external reference beam, resulting in a very simple and robust registration setup. Based on this approach, a lensless coherent microscope has been realized, in which the complex amplitude has been experimentally registered inside a 3 mm aperture in a grid with 150x150 sampling points. The experimentally registered field have been propagated in a virtual optical system to demonstrate virtual imaging, digital focusing, and adaptive correction.

The work of M. Verhaegen, G. Vdovin, P. Pozzi and O. Soloviev is supported by the European Research Council, Advanced Grant Agreement No. 339681. The work of O. Soloviev and G. Vdovin is partly supported by the program “5 in 100” of the Russian Ministry of Education. The work of Hai Gong is sponsored by the China Scholarship Council.

References

- [1] M K Kim. *Digital Holographic Microscopy*. Springer, 2011.
- [2] Ichirou Yamaguchi and Tong Zhang. Phase-shifting digital holography. *Opt. Lett.*, 22(16):1268–1270, Aug 1997.
- [3] Tong Zhang and Ichirou Yamaguchi. Three-dimensional microscopy with phase-shifting digital holography. *Opt. Lett.*, 23(15):1221–1223, Aug 1998.
- [4] N. G. Vlasov, S. G. Kalenkov, D. V. Krilov, and A. E. Shtanko. Non-lens digital microscopy. *Proc. SPIE*, 5821:158–162, 2005.
- [5] Gabriel Popescu, Lauren P Deflores, Joshua C Vaughan, Kamran Badizadegan, Hidenao Iwai, Ramachandra R Dasari, and Michael S Feld. Fourier phase microscopy for investigation of biological structures and dynamics. *Opt. Lett.*, 29(21):2503–2505, 2004.
- [6] Gabriel Popescu, Takahiro Ikeda, Ramachandra R Dasari, and Michael S Feld. Diffraction phase microscopy for quantifying cell structure and dynamics. *Opt. Lett.*, 31(6):775–777, 2006.
- [7] Björn Kemper, Angelika Vollmer, Christina E Rommel, Jürgen Schnekenburger, and Gert von Bally. Simplified approach for quantitative digital holographic phase contrast imaging of living cells. *J. Biomed. Opt.*, 16(2):026014, 2011.
- [8] R. W. Gerchberg and W. O. Saxton. A practical algorithm for the determination of phase from image and diffraction plane pictures. *Optik*, 35:237, 1972.
- [9] Jianwei Miao, Pambos Charalambous, Janos Kirz, and David Sayre. Extending the methodology of X-ray crystallography to allow imaging of micrometre-sized non-crystalline specimens. *Nature*, 400(6742):342–344, 1999.
- [10] Stefan Witte, Vasco T Tenner, Daniel WE Noom, and Kjeld SE Eikema. Lensless diffractive imaging with ultra-broadband table-top sources: from infrared to extreme-ultraviolet wavelengths. *Light Sci Appl*, 3:e163–, March 2014.
- [11] Roland Shack and Ben C. Pratt. History and principles of Shack-Hartmann wavefront sensing. *Journal of Refractive Surgery*, 17:573–577.
- [12] Pierre Bon, Guillaume Maucort, Benoit Wattellier, and Serge Monneret. Quadriwave lateral shearing interferometry for quantitative phase microscopy of living cells. *Opt. Express*, 17(15):13080–13094, 2009.
- [13] G Indebetouw, P Klysubun, T Kim, and T C Poon. Imaging properties of scanning holographic microscopy. *J. Opt. Soc. Am. A*, 17(3):380–390, 2000.
- [14] Edmund Y Lam, Xin Zhang, Huy Vo, Ting-Chung Poon, and Guy Indebetouw. Three-dimensional microscopy and sectional image reconstruction using optical scanning holography. *Appl. Opt.*, 48(34):H113–H119, 2009.
- [15] Dana Dudley, Walter M. Duncan, and John Slaughter. Emerging digital micromirror device (dmd) applications. *Proc. SPIE*, 4985:14–25, 2003.
- [16] M. Sheikh and Nabeel A. Riza. Demonstration of pinhole laser beam profiling using a digital micromirror device. *Photonics Technology Letters, IEEE*, 21(10):666–668, May 2009.
- [17] J. Romberg. Imaging via compressive sampling. *Signal Processing Magazine, IEEE*, 25(2):14–20, March 2008.